

Average crossing number of Gaussian and equilateral chains with and without excluded volume

P.M. Diesinger^{1,a} and D.W. Heermann²

¹ Institute of Theoretical Physics, Heidelberg University, 69118 Heidelberg, Germany

² Institute of Theoretical Physics and Interdisziplinäres Zentrum für Wissenschaftliches Rechnen der Universität Heidelberg, 69118 Heidelberg, Germany

Received 9 November 2007 / Received in final form 1st February 2008

Published online 11 April 2008 – © EDP Sciences, Società Italiana di Fisica, Springer-Verlag 2008

Abstract. We study the influence of excluded volume interactions on the behaviour of the mean average crossing number (mACN) for random off-lattice walks. We investigated Gaussian and equilateral off-lattice random walks with and without ellipsoidal excluded volume up to chain lengths of $N = 1500$ and equilateral random walks on a cubic lattice up to $N = 20000$. We find that the excluded volume interactions have a strong influence on the behaviour of the local crossing number $\langle a(l_1, l_2) \rangle$ at very short distances but only a weak one at large distances. This behaviour is the basis of the proof in [3,7] for the dependence of the mean average crossing number on the chain length N . We show that the data is compatible with an $N \ln(N)$ -behaviour for the mACN, even in the case with excluded volume.

PACS. 61.82.Pv Polymers, organic compounds

1 Introduction

The mean average crossing number (mACN) was introduced in [1,2] as a simplified version of the writhe of a random walk. For a given linear closed polymer the crossing number associated with a particular projection of the random walk is the number of crossings one observes when the polymer is projected to a plane under the given projection direction. The average crossing number (ACN) of the polymer is then defined as the average of this crossing number over all possible projection directions [3]. The mean average crossing number (mACN) is the average of the ACN over all possible random walks of a certain length N . Diaó suggested to use the mACN, which was called ‘entanglement complexity’ in a previous work [4], as a measure of entanglement to determine whether a (closed) polymer chain is highly or weakly knotted [5]. Grassberger [6] showed that the mACN is mainly a measure for the ‘opacity’ of a random walk.

For equilateral and for Gaussian random walks without excluded volume Diaó [3,7] succeeded in showing that the mean average crossing number behaves $c_1 N \ln N + c_2 N$. In [1,2] it was shown that the mACN satisfies $\text{mACN} \propto N^\alpha$ for $N \rightarrow \infty$ with $\alpha \approx 1.2$ [8].

In the next section we investigate the behaviour of the mACN of equilateral and Gaussian random walks with and without excluded volume. Chains without excluded

volume interactions are called ‘phantom chains’ in the text.

2 The mean average crossing number

We start by investigating the effects of excluded volume interactions on the mean average crossing number (mACN) of equilateral and Gaussian random walks which represent polymer classes. A *Gaussian Random vector* $\vec{v} = (x, y, z)$ is a random point with coordinates x, y and z which are independent standard normal variables (with means = 0 and variance = 1). A *Gaussian random walk (or chain)* of n steps consists of $n+1$ points $X_{\{0 \dots n\}}$ such that $X_{k+1} - X_k$ ($k = 0, 1, \dots, n-1$) are Gaussian random vectors and $X_0 = (0, 0, 0)^t$.

A vector $U = (u, v, w)^t$ is called *uniformly distributed on the unit sphere* S^2 , if the probability density function of U is $\varphi(U) = \frac{1}{4\pi}$ for $|U| = 1$ and $\varphi(U) = 0$ otherwise. If U_1, U_2, \dots, U_n are n independent random vectors uniformly distributed on S^2 , then an *equilateral random walk (or chain)* is defined as the sequence of the points $X_0 = O, X_k = \sum_{i=1}^k U_i, k = 1, 2, \dots, n$ in \mathbb{R}^3 .

A hard-core ellipsoidal potential was used to simulate the excluded volume interactions of the chain segments since many polymers can be modeled by such a potential (cf. Fig. 1).

^a e-mail: p.m.diesinger@gmx.de

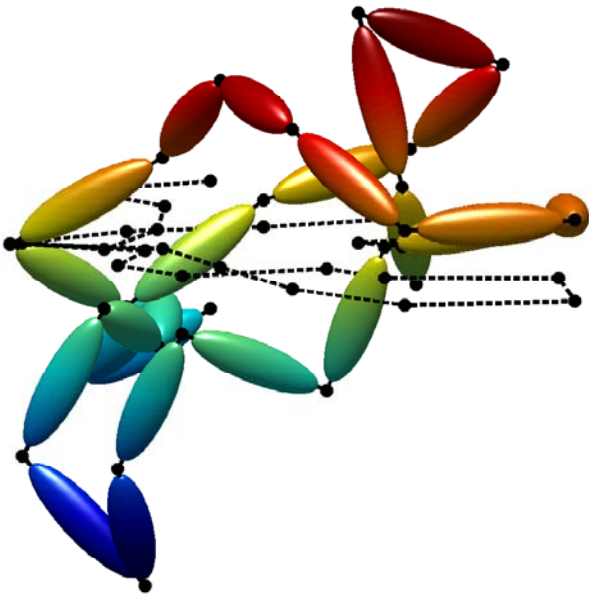


Fig. 1. An example for an equilateral chain of length $N = 25$ with excluded volume. The dashed line is the projection of the chain onto the xy -plane and shows seven crossings. The average crossing number of this particular chain is $\text{ACN} \approx 5.29$ and the mean average crossing number of all equilateral chains of length 25 is 3.13. The grayscale gives the height of the ellipsoids.

To understand the effect of the excluded volume interaction, let us focus our attention initially on the scale invariant

$$a(l_1, l_2) = \frac{1}{2\pi} \int_{\gamma_1} \int_{\gamma_2} \frac{|\dot{\gamma}_1(t), \dot{\gamma}_2(s), \gamma_1(t) - \gamma_2(s)|}{\|\gamma_1(t) - \gamma_2(s)\|^3} dt ds \quad (1)$$

which is the basis for the prediction [3,7]

$$\text{mACN}_{\text{Gaussian}}(N) = \frac{1}{2\pi} N \ln(N) + O(N) \quad (2)$$

$$\approx \frac{1}{2\pi} N \ln(N) + c_1 N \quad (3)$$

$$\text{mACN}_{\text{equilateral}}(N) = \frac{3}{16} N \ln(N) + O(N) \quad (4)$$

$$\approx \frac{3}{16} N \ln(N) + c_2 N \quad (5)$$

for the phantom and equilateral chains of length N without excluded volume. In the above l_1 and l_2 are segments of the chain and γ is the arc-length parametrization (the above invariant can be considered as the first element in a hierarchy [9,10]).

In [3,7] it was shown that for two chain segments l_1, l_2 on average $a(l_1, l_2)$ behaves as

$$\langle a(l_1, l_2) \rangle = \frac{1}{2\pi d^2} + O\left(\frac{1}{d^{2.5}}\right) \quad (6)$$

for Gaussian phantom and

$$\langle a(l_1, l_2) \rangle = \frac{1}{16d^2} + O\left(\frac{1}{d^3}\right) \quad (7)$$

for equilateral phantom chains, where d is the (fixed) distance between the two considered chain segments l_1 and l_2

and $a(l_1, l_2)$ is averaged over all possible orientations of l_1 and l_2 . So far no prediction has been derived for the case of chains with excluded volume interaction. Hence it is important to ask how far the estimate also applies to the case of excluded volume interaction and how differences manifest themselves.

Using Monte Carlo simulations [11,12] we calculated the average crossing number by counting the crossings in numerous projections of γ and taking the average over all these crossing numbers. For every calculated average crossing number, we averaged over 1000 randomly chosen planes to obtain a good estimate of the actual ACN value.

Four types of chains have been investigated by us: Gaussian and equilateral chains with and without excluded volume. All chains are open and start at the origin. The excluded volume chains were generated with an (off-lattice) Pivot-Algorithm, which for example can be found in [18]. We used a hard-core excluded volume potential, in order to speed up the simulations. Between two consecutive chain points there is an ellipsoidal hard-core excluded volume (cf. Fig. 1). When generating chains with excluded volume interactions the Pivot-Algorithm simply rejects all chain conformations which have at least two overlapping ellipsoids.

Roughly speaking the mACN depends on two quantities: the behaviour of $\langle a(l_1, l_2) \rangle$ in dependence of d and the probability distribution (pdf) of d . To understand the effects on the mACN due to excluded volume, it is necessary to understand how excluded volume interactions affect these two parameters.

For $\langle a(l_1, l_2) \rangle$ we find that the excluded volume interactions do not have any measurable effect for distances larger than two (equilateral case) or three (Gaussian case) chain segments (see Fig. 2). A calculation of correlation lengths for the orientation of the chain segments leads to similar results, namely $d_c \approx 1.39$ for equilateral and $d_c \approx 2.81$ for Gaussian chains. Each point of Figures 2, 3 and 4 for $\langle a(l_1, l_2) \rangle$ is an average over at least 10^4 points. The dashed lines in this Figure show the leading order term for the theoretical prediction of [3,7] (cf. Eqs. (6) and (7)). Although these predictions have been calculated to describe the behaviour of $\langle a(l_1, l_2) \rangle$ for large d , they already fit very well for $d > 1$ for chains with and without excluded volume. Therefore they might be used to derive some estimations of the mACN behaviour for chains *with* excluded volume, too (only the large d case is important here, because these chains contribute mostly to the mACN).

There seems to be a discontinuity at $d = 0$, since $\langle a(l_1, l_2) \rangle$ should vanish at the origin according to the Gauss invariant [3,7]. Figure 3 shows the comparison of our numerical results with the theoretical prediction of the papers cited above. One can see, that the predicted behaviour is not only good in the case of phantom chains but also in the case of chains with excluded volume.

In contrast to $\langle a(l_1, l_2) \rangle$ there is a huge effect of the excluded volume interactions on the probability distributions of d which can be seen in Figure 4 for equilateral and Gaussian chains of length $N = 100$ (together with

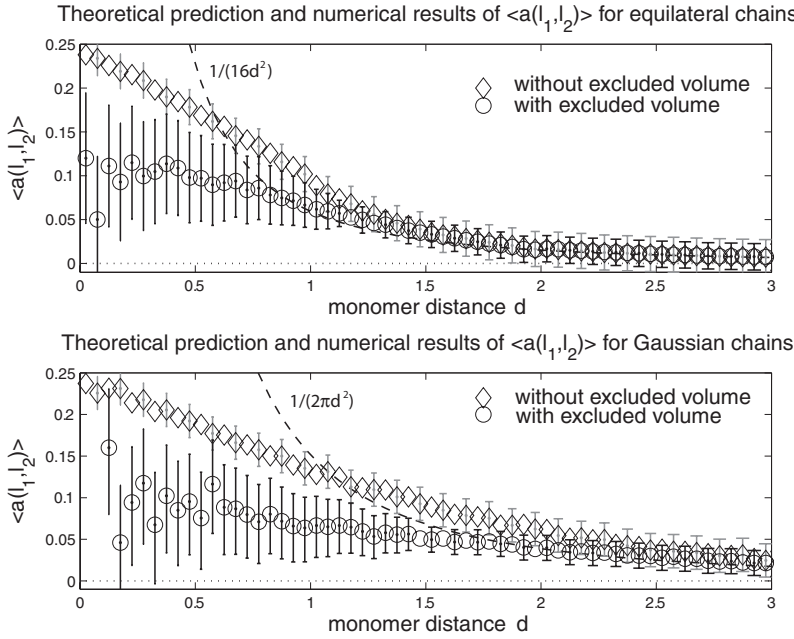


Fig. 2. The leading order term for the theoretical prediction of the large d case [3,7] and the numerical results for $\langle a(l_1, l_2) \rangle$ of Gaussian and equilateral chains for small values of d . One can roughly see that $\langle a(l_1, l_2) \rangle$ is discontinuous at $d = 0$. Every data point represents an average over at least 10^4 values.

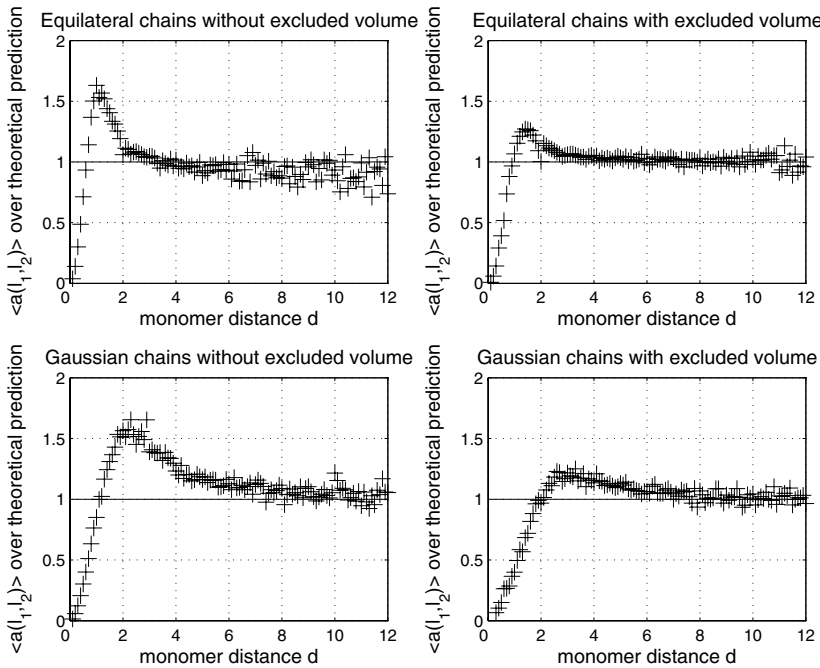


Fig. 3. Shown are the ratios between the prediction for the leading order term for the invariant $\langle a(l_1, l_2) \rangle$ and the simulation results. While the prediction pertains to chains without excluded volume the results show the agreement with the theoretical predictions are excellent for distances larger than 10 for chains with and without excluded volume. The strong fluctuations at the end for the larger distances are a consequence of the plotted ratio. A single point in the figure represents at least an average over 10 000 simulation results.

the numerical results for $\langle a(l_1, l_2) \rangle$ on a larger scale in the background of the figure). One can see that the chains with excluded volume are much more stretched as expected due to the enhanced value of ν for the radius of gyration than those without. The Gaussian chains are longer than the equilateral ones. This is a consequence of the Gaussian probability distribution since the mean length of Gaussian chain segments is about 1.6 and the length of all equilateral chain segments is normalized.

The pdfs of the equilateral chains show peaks at $d \approx 2$. This is a feature of the equilateral chains since the distance of the endpoints of two consecutive line segments is always larger than 0 and smaller than 2. If d exceeds 2,

the probability to find monomers with a distance d drops immediately. In the case of the equilateral chains with excluded volume the end to end distance of two consecutive line segments is always larger than

$$d_{\min} = \sin\left(\frac{\alpha_{\min}}{2}\right) = 0.66 \quad \text{with } \alpha_{\min} = 83.62 \text{ degrees,}$$

where the minimal value of the angle α between two consecutive chain segments is determined by our ellipsoidal excluded volume model. The pdf of the equilateral chains *with* excluded volume has two discontinuity points (at $d_{\min} = 0.66$ and $d = 2$, cf. Fig. 4). The one *without* excluded volume shows only the one at $d = 2$ as explained above.

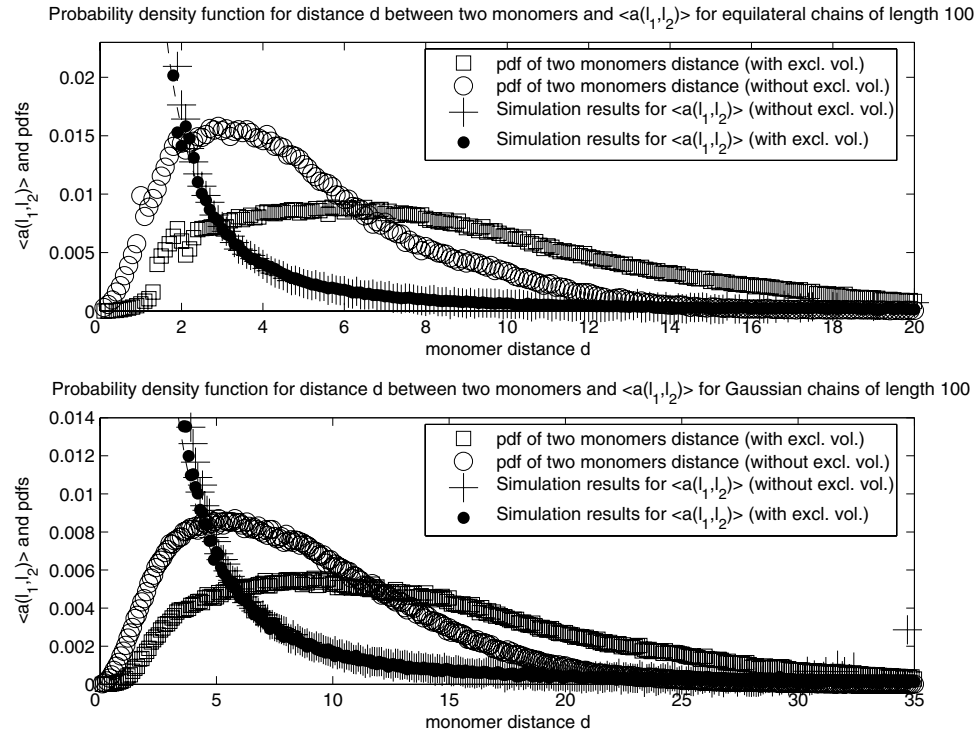


Fig. 4. Shown are the distance probability density functions (pdf) for Gaussian and equilateral chains with the cases of non-and excluded volume. In both cases the distribution is rather different but yield the same behaviour on average (cf. Fig. 3).

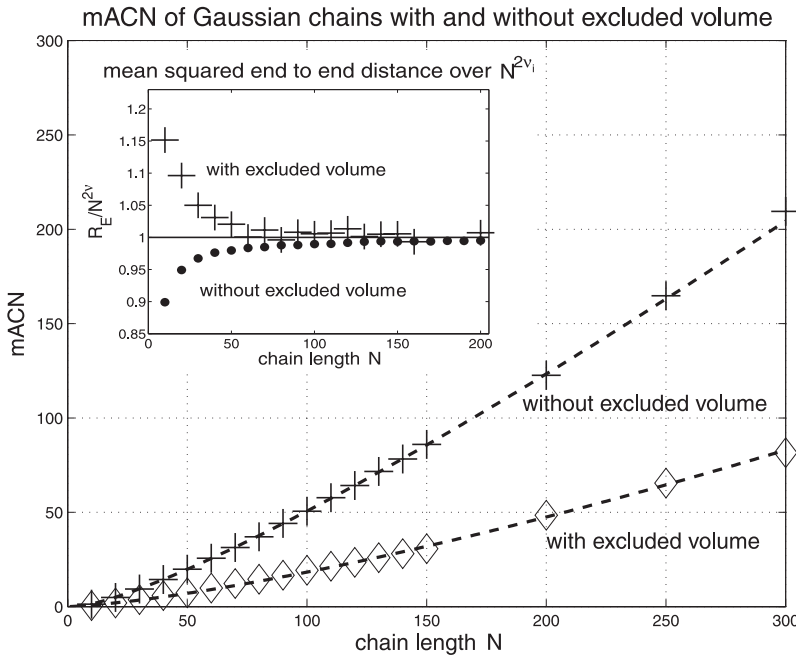


Fig. 5. Shown are the mACN for Gaussian chains with and without excluded volume and the best fit for each one (cf. Tabs. 1 and 2). The inset shows the end-to-end distance for the equilateral chains over its theoretical prediction $N^{2\nu_1}$ ($\nu_1 = 0.5$ and $\nu_2 = 0.588$). As this ratio converges to one, one can see that the end-to-end distance follows the expected behaviour. Every data point of the inset represents an average over at least 10^4 points, and every point of the main figure is an average of at least 10^5 points.

Figures 5 and 6 show that the total mACN for chains with excluded volume is much lower than for phantom chains. As pointed out above this is mainly a consequence of the much broader distance pdf for chains with excluded volume. The orientation effects (i.e. the changes of $\langle a(l_1, l_2) \rangle$) play only a minor role. As these random walks are a model for equilibrated polymers in solution and as these polymers do have excluded volume interactions one should expect a much lower ACN for these polymers than predicted by [3,7]. Furthermore, a linear correction term

to the predicted $N \ln N$ -behaviour (cf. Fig. 7) seems to worsen the fits in the case of the chains with excluded volume, as early points are all above the dashed line and late points are below the line. Each data point in the Figures, which show the mACN, is an average over at least 10^5 points.

The prediction for the mACN by Diao et al. [3,7] as stated in equations (3) and (5) are in good agreement with our simulations. Our simulation results confirm these results, and we calculated a factor of $c_2 = -0.3051$ for the

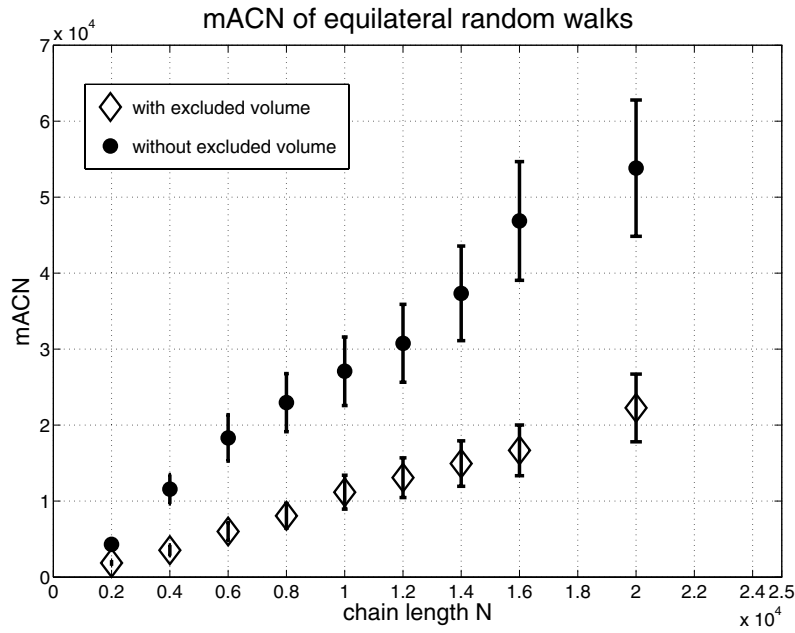


Fig. 6. The mACN of equilateral random walks on a cubic lattice with and without excluded volume interactions.

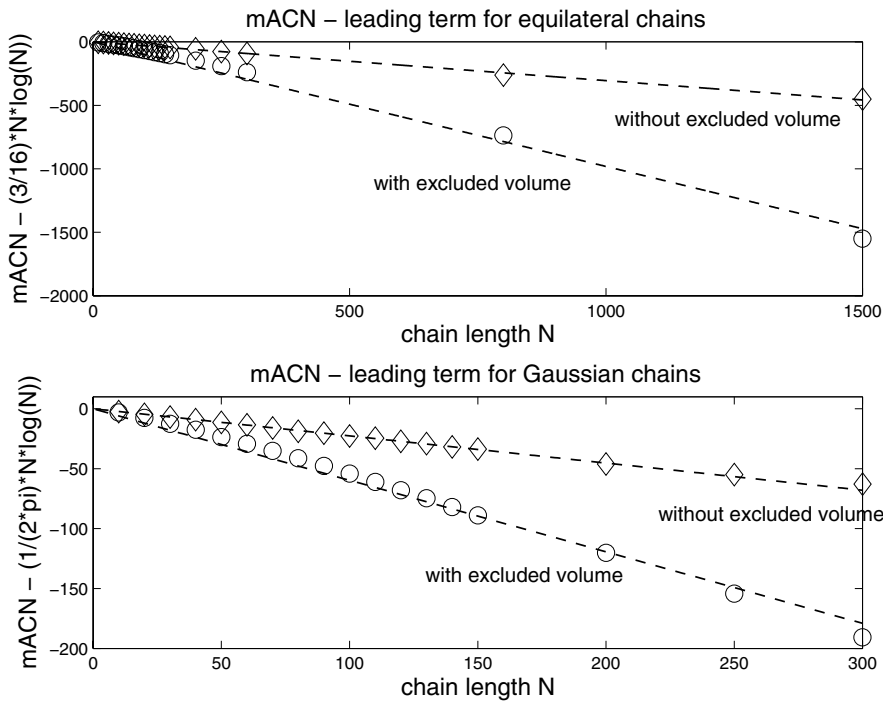


Fig. 7. The error term of the theoretical prediction of the mean average crossing number is negative and much smaller for the chains with excluded volume. Every data point represents again an average over at least 10^5 points.

equilateral chains and a factor of $c_1 = -0.2265$ for the Gaussian ones.

The fit results are compiled in the following two tables. Please note that the data for the equilateral chains with excluded volume reaches up to $N = 1500$ for off-lattice chains and up to $N = 20000$ for chains on a cubic lattice, whereas the mACN for the Gaussian chains reaches to $N = 300$ (off-lattice). The summed square of residuals (sse) and the coefficient of multiple determination (rsquare) are also given in Tables 1 and 2. The power

Table 1. Different data fits.

chains without excluded volume				
data	fit	a	sse	rsquare
equilateral	$(3/16)N \ln(N) + aN$	-0.3051	445.2	0.9998
Gaussian	$(1/2\pi)N \ln(N) + aN$	-0.2265	61.4	1.0000

law fits with $b > 1$ will beat $n \ln(n)$ for large n . They are shown here to give an approximation of the mACN for smaller chains.

Table 2. Fitting parameters.

Gaussian chains with excluded volume				
fit	a	b	sse	rsquare
aN^b	0.03239	1.376	10.07	0.9988
$(1/2\pi)N \ln(N) + aN$	-0.5968	—	537.53	0.9349
$aN \ln(N) + bN$	0.07468	-0.1553	16.3505	0.9980
$(1/2\pi)N \log(N)^a$	0.2426	—	310.4	0.9624
equilateral chains with excluded volume				
aN^b	0.06382	1.232	1306.1	0.9952
$(3/16)N \ln(N) + aN$	-0.9812	—	29987	0.8896
$aN \ln(N) + bN$	0.03914	0.05466	241.58	0.9991
$(3/16)N \log(N)^a$	0.2902	—	1010.1	0.9963

3 Discussion

Our results in the first part show that the topological invariant and the behaviour of $\langle a(l_1, l_2) \rangle$, which are the basis for the proof by Diao [3,7] and co-workers, are weakly influenced by excluded volume interactions. Hence it is still unclear, especially in the light of the inconclusive simulation data, whether the proven law $c_1 N \ln N + c_2 N$ for the non-excluded volume case changes to a power law, as suggested by [1,2]. Much larger chains are needed to clearly discern between the possibilities. A rough estimate shows that we need chains that are at least ten times longer. Here the problem is that despite the well-developed Pivot algorithm the computation of the excluded volume interaction is so time-consuming that for now it seems to be possible to do such a calculation only expending a truly fair amount of computing resources.

We are very grateful to J. Odenheimer and K. Binder for discussions.

References

1. E. Orlandini, M.C. Tesi, S.G. Whittington, D.W. Summers, E.J. Janse van Rensburg, *J. Phys. A: Math. Gen.* **27**, L333 (1994)
2. E.J. Janse van Rensburg, D.W. Summers, E. Wassermann, S.G. Whittington, *J. Phys. A: Math. Gen.* **25**, 6557(1992)
3. Y. Diao, A. Dobay, R.B. Kusner, K. Millett, A. Stasiak, *J. Phys. A: Math. Gen.* **36**, 11561 (2003)
4. A.L. Kholodenko, D.P. Rolfsen, *J. Phys. A: Math. Gen.* **29**, 5677(1996)
5. Y. Diao, *J. Knot Theo. Rami* **4**, 189 (1995)
6. P. Grassberger, *J. Phys. A: Math. Gen.* **34**, 9959 (2001)
7. Y. Diao, C. Ernst, *Physical and Numerical Models in Knot Theory Including Applications to the Life Sciences*, edited by, J.A. Calvo, K.C. Millett, E.J. Rawdon, A. Stasiak (World Scientific Publishing, Singapore, 2005), pp. 275–292
8. G.A. Arteca, *Phys. Rev. E* **49**, 2417(1994)
9. E. Guadagnini, *The Link Invariants of the Chern-Simons Field Theory* (Walter de Gruyter, Berlin,1993)
10. E. Witten, *Commun. Math. Phys.* **121**, 351 (1998)
11. D.W. Heermann, *Computer Simulation Methods in Theoretical Physics*, 2nd edn. (Springer Verlag, Heidelberg, 1990)
12. K. Binder, D.W. Heermann *Monte Carlo Simulation in Statistical Physics*, 4th edn. (Springer, Heidelberg, 2002)
13. C.L. Adams, *The knot book* (Freeman, New York, 1994)
14. G. Calugareanu, *Rev. Math. Pures Appl. (Bucarest)* **4**, 5 (1995)
15. A. Dobay, Y. Diao, J. Dubochet, A. Stasiak, Scaling of the average crossing number in equilateral random walks, knots and proteins, in *Series on Knots and Everything* (World Scientific, 1988)
16. O. Farago, Y. Kantor, M. Kardar, *Europhys. Lett.* **60**, 53 (2002)
17. L.H. Kauffman, *Knots and Physics* (World Scientific, Singapore, 1993)
18. N. Madras, A. Sokal, *J. Stat. Phys.* **50**, 109 (1988)